Nordic Hydrology, 34 (3), 2003, 245-266

Investigation of Ice and Water Properties and Under-ice Light Fields in Fresh and Brackish Water Bodies

Matti Leppäranta
Div. of Geophysics, Univ. of Helsinki, Finland
A. Reinart, A. Erm, H. Arst,
M. Hussainov and L. Sipelgas
Marine Systems Inst., Tallin Tech. Univ., Estonia

Light transmission through ice and light conditions beneath ice have been investigated in the mild winter of the year 2000 in eight Estonian lakes and in one brackish water basin, Santala Bay in the Gulf of Finland. A new system designed for optical measurements beneath the ice was successfully tested. In the water body the vertical profiles of photosynthetically active radiation (PAR), temperature and oxygen were mapped. The concentrations of optically active substances (dissolved organic matter, chlorophyll *a*, particles) were estimated for water samples and meltwater of ice samples. The PAR band albedo was 0.28-0.76 and transmittance was 1-52% for the ice/snow cover. The light field below ice was much more diffuse than in open water conditions. Euphotic depth was 0.1-5.5 m. The amount of yellow substance in lake ice is very small in comparison with the lake water; lake ice may contain a lot of particles, but their source is atmospheric fallout rather than the water body. In some lakes a depletion of oxygen was observed. There were considerable differences between the fresh and brackish water ice (structure, stratigraphy, amount of impurities), which influenced the underwater light field.

Introduction

Lake ice cover forms a barrier between the atmosphere and the water body, and it plays a major role in lake ecosystems by affecting on the volume of liquid water, mixing, sedimentation, aeration and light conditions. It has been shown that the ice

cover affects phytoplankton photosynthesis in water and therefore also the vertical distribution of nutrients and living organisms (Fritsen and Priscu 1999). However, in general the links between ice geophysics and ecological processes in lakes have not been well quantified.

In Estonian lakes and the coastal waters of Gulf of Finland the winters are characterised by a pronounced diversity. Snow and ice are products of cold weather and precipitation, and therefore they vary widely from the fresh stages in autumn to the spring melting season as well as from year to year in their thickness and properties (temperature, crystal structure, transparency, albedo, impurities, *etc.*) (Michel and Ramseier 1971; Perovich 1998; Granberg 1998). Lake ice is also different in quality from brackish ice, which contains brine channels where phytoplankton may grow.

Several studies have been performed on the snow and ice of Estonian lakes and the Baltic Sea (*e.g.*, Palosuo 1963; Tooming and Kadaja 1995; Leppäranta *et al.* 1998). The optical properties of ice have been mostly investigated for the Arctic and Antarctic sea ice (*e.g.*, Arrigo *et al.* 1991; Allison *et al.* 1993; Perovich 1998). Field investigations on the optical properties of Baltic Sea ice commenced in 1998 (Rasmus *et al.* 2002) but in Estonian lakes such work has not been done prior to this study.

The present paper reports the results of a pilot study on the optics of ice and snow and the under-ice light field in Estonian lakes, with comparisons with a brackish water basin (Santala Bay in the Gulf of Finland, with a salinity of about 5‰). A new measurement system was designed and tested for the under-ice radiation measurements. The data consist of irradiances, optically active substances (OAS) in ice and water, and the temperature and dissolved oxygen in the water. They aid the understanding of the ice melting process and the wintertime ecological conditions in lakes.

Materials and Methods

Data Collected

The period of field measurements was January 18 to March 30, 2000, when the ice was safe enough for the work. Eight Estonian lakes and Santala Bay in the Gulf of Finland were investigated. The lakes span the range of trophic states, from oligotrophic to dystrophic, in the region 58°-60° N × 24°-27° E, and Santala Bay (at about 60° N, 23° E) is a small basin in the fast ice zone (Table 1). For the solar radiation, spectral measurements were made from samples and PAR-band (photosynthetically active radiation, 400-700 nm) *in situ* plane (vector) and scalar irradiance measurements were made in the field. The data obtained consist of

1) Snow and ice thickness;
2) Structure (stratigraphy, crystals) of ice, based on thick and thin sections;
3) The concentration of chlorophyll *a* (C_{chl}) and the spectral (350-700 nm) attenua-

Table 1 – Description of ice cover and water type of investigated basins in winter 2000.

Basin	Date	Water type	Ice thickness	Surface conditions
Lake Maardu	18 Jan	Meso-	16 cm	Grey and smooth ice
	8 Mar	trophic	28 cm	Snow patches on grey and rough ice
Lake Harku	19 Jan	Eu-	14 cm	Grey and smooth ice
	3 Feb	trophic	22 cm	2 cm snow on grey and rough ice
Lake Ülemiste	4 Feb	Eu-	22 cm	2-6 cm snow on grey and rough ice
	15 Feb	tro-	27 cm	1-2 cm snow on the ice
	23 Mar	phic	26 cm	Grey and slightly rough ice
Lake Paukjärv	23 Feb	Oligo-trophic	21 cm	6 cm snow on grey and smooth ice
Lake Verevi	28 Feb	Meso-trophic	22 cm	0.4 cm water on smooth ice
Lake N. Valgjärv	29 Feb	Meso-trophic	19 cm	1-2 cm water on smooth ice
Lake N. Mustjärv	29 Feb	Dys-trophic	16 cm	1 cm water on smooth ice
Lake Võrtsjärv	1 Mar	Eu-trophic	30 cm	0.5 cm water on smooth ice with dark and white patches
Santala Bay	15 Mar	Oligo-	27-29 cm	Dry, grey and slightly rough ice
	16 Mar	meso-	27-29 cm	Dry shiny and slick ice
	17 Mar	trophic;	27-29 cm	Patches of fresh snow on smooth ice
	18 Mar	brackish water	27-29 cm	Patches of dirty snow on smooth and slick ice
	28 Mar		22 cm	Patches of hoarfrost and snow on white and smooth ice
	29 Mar		15 cm	~10 cm width crack covered by transparent ice across whitish ice sheet
	30 Mar		21 cm	Melting grey, soft and rough ice

tion coefficient of filtered and unfiltered ice meltwater (c^*_f and c^*), in some cases these were done separately for different ice layers;

4) The concentrations of chlorophyll *a* and suspended matter (C_s), and the spectral attenuation coefficient of filtered and unfiltered water samples from different depths (z) under the ice;
5) Incident plane quantum PAR irradiance (E_d (0+));
6) Plane downwelling and scalar quantum PAR irradiances in the water at different depths below the ice cover ($E_d(z)$ and $E_o(z)$); and
7) Vertical profiles of temperature (t) and dissolved oxygen (O_2) in the water body.

Our data bank is rather irregular: in some cases all measurements were made, including some for different ice layers: Maardu (8 March), Ülemiste (15 Feb and 23 March), Paukjärv, Verevi, Nohipalu Valgjärv, Võrtsjärv, and Santala Bay (16 and 28 March). The Santala radiation data were also used to estimate the spectral albedo (α) and PAR albedo (α_{PAR}).

Properties of Water and Ice Meltwater

Water samples were usually taken from depths of 0.1, 1, 2, and 4 m beneath the ice. Ice cores (cross-section 15 cm × 15 cm) were taken with a drill and a saw close to the sites of the irradiance measurements. They were horizontally sliced into pieces, which were melted before analysis.

The concentration of suspended matter was determined by its dry weight after filtration of the water through cellulose acetate filters (Millipore, pore diameter 0.45 μm); at least 1/2 liter of water was filtered. For chlorophyll *a*, seston water was filtered on Whatman GF/C filters. Pigments were extracted with ethanol and analyzed by a standard spectrophotometrical method at 665 nm. The spectra (350-700 nm) of c^* and c_f^* were determined from water samples by laboratory spectrophotometer Hitachi U1000. The measured quantity is $c^* = c - c_d$, where c and c_d are, respectively, the beam attenuation coefficients of the water sample and distilled water; the values were not corrected for small-angle forward scattering. The PAR attenuation coefficient was integrated from the spectral data. The spectral and PAR attenuation coefficients are rather good indicators of the transparency and quality of water (Arst *et al.* 1996, 1999b). In filtered water the attenuation coefficient is close to the absorption coefficient of yellow substance because the contribution of scattering is small; here the attenuation coefficient at 380-nm is used to estimate the concentration of yellow substance. There were altogether 20 vertical profiles of temperature and dissolved oxygen measured using the oxymeter *MARVET-JUNIOR, Estonia.*

For the ice meltwater the results about the concentration of suspended matter are not used here because they contained inconsistencies, which need further investigations. A major question is whether the freezing-melting cycle changes the properties of impurities in natural waters. A series of experiments on frozen and melted samples (the water samples were frozen for 8-10 days) from the turbid fresh water of Pärnu River and the brackish water of Pärnu Bay resulted in a huge increase (88-400%) of the concentration of suspended matter (Arst *et al.* 1999a). We repeated this experiment using water samples from lakes Ülemiste, Harku and Maardu in winter 2000. The results for Lake Ülemiste showed good agreement with the previous investigation but for the other lakes the freezing-melting process did not have much influence. Surprisingly, while the concentration of suspended matter increased in the Lake Ülemiste sample, there was no change in the PAR-band attenuation coefficient. To estimate the particle size distribution we filtered the sample through filters with the pore sizes of 8, 5, 3, 0.45 and 0.22 μm. More than 95% (by weight) of the material was retained in the 8-μm filter. However, the effect of the freezing-melting cycle

on the impurities remains unknown, and a wider set of experiments has to be performed.

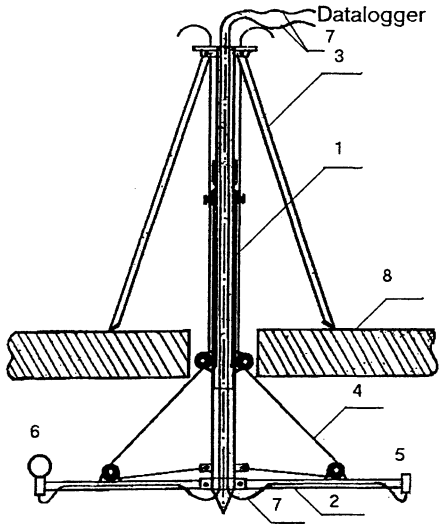

Fig. 1. Device for measuring the plane and scalar irradiances in the water under the ice cover: (1) telescopic probe, (2) console, (3) tripod, (4) cord, (5) plane sensor (LI-192 SA), (6) spherical sensor (LI-193 SA), (7) underwater cable and (8) ice layer.

Radiation Measurements

For the PAR measurements under ice cover, a special device was constructed (Fig. 1). The consoles (2) are first alongside the telescopic probe (1). Then the device is lowered into the water through a 30 cm hole in the ice and fastened on the tripod (3). Then consoles are positioned horizontally using cords (4). By changing the length of the probe and the inclination of the legs of the tripod, the desired measurement depth can be selected. The system allows irradiance measurements to about 1 m from the ice-hole in the horizontal direction down to a depth of 1.5 m.

Two PAR sensors (*LI-COR*, inc. USA) were used: LI-192 SA (plane irradiance) and LI-193 SA (scalar irradiance). Downwelling plane irradiance is the irradiance coming onto a plane surface from the upper hemisphere while scalar irradiance is the irradiance coming onto a sphere (*e.g.*, Jerlov 1968). Both sensors have been separately calibrated for quantum irradiance. In the air the quantum irradiance of 4.6 μmol s^{-1} m^{-2} corresponds to a radiative energy of 1 W m^{-2} but in the water this relationship depends on water properties (Reinart *et al.* 1998). Incident PAR was measured with the LI-192 SA sensor simultaneously with the underwater measurements.

The instrument was first lowered into the water and then brought back to the surface, recording was done in both directions. To examine the patchiness in the optical properties of ice cover the procedure was repeated at other locations.

Transmission of PAR through the snow and ice is taken as the ratio of transmitted to incident irradiance. Depth averaged plane and scalar diffuse attenuation coefficients of water (K_d(PAR) and K_o(PAR)), defined by the exponential attenuation laws for plane and scalar irradiance, respectively, were obtained using the least-squares method from the vertical irradiance profiles; the coefficient of determination was always greater than 0.96 in the regression.

The albedo was estimated from ST 1000 spectrophotometer (*Ocean Optics*, inc. USA) data, adjusted for out-door measurements (Kutser *et al.* 1999). The downwelling and upwelling spectral irradiances were measured simultaneously with 2π cosine collectors over the band 350-850 nm. Under low light conditions upwelling irradiance above a wavelength of 700 nm may be influenced by the insufficient sensitivity of the sensor. For the PAR band albedo was obtained by integration from the spectral data.

Properties of Ice and Water

Ice Surface and Structure

Winter 2000 was mild with not much snowfall in the study region (GLOBE database; http://www.globe.gov/). An especially uncommon feature was the mildness of February: the mean midday temperature was +0.7 °C while the long-term average is -6 °C (Russak 1990). Lakes froze over in December 1999. In January the ice was mostly snow free and its thickness was around 15 cm (Table 1). During the lake observation period (18 Jan-30 March) the ice thickness was 14-30 cm, and only in four cases in February was there any snow cover (1-6 cm). The ice surface was slightly rough under the snow while dry bare ice was mostly smooth and looked grey. Toward the end of February a thin water layer formed on the ice due to the snow melting. Apart from Lake Võrtsjärv our lakes are relatively small, and the snow and ice cover seemed to be homogeneous.

The vertical structure of the ice sheet had clear and opaque layers. Lake Verevi ice (Fig. 2a) had a typical lake ice sheet structure. On top there was opaque snow-ice (5 cm) and beneath that clear congelation ice (17 cm). There were many large (diameter up to 5 mm) gas bubbles inside the congelation ice. More complicated cases were also found: In Lake Võrtsjärv (Fig. 2b) there was a snow-ice layer on top (3 cm) and a lower opaque layer at depths of 18-22 cm, possibly frazil ice; Lake Maardu (Fig. 2c) ice had a 3-cm opaque top layer and another opaque layer at 9-17 cm with many gas bubbles, probably due to gas release from the water body or bottom plants.

Thin sections were prepared to examine the crystal structure of ice in polarized light. The result showed typical lake ice features: the snow-ice layer consisted of

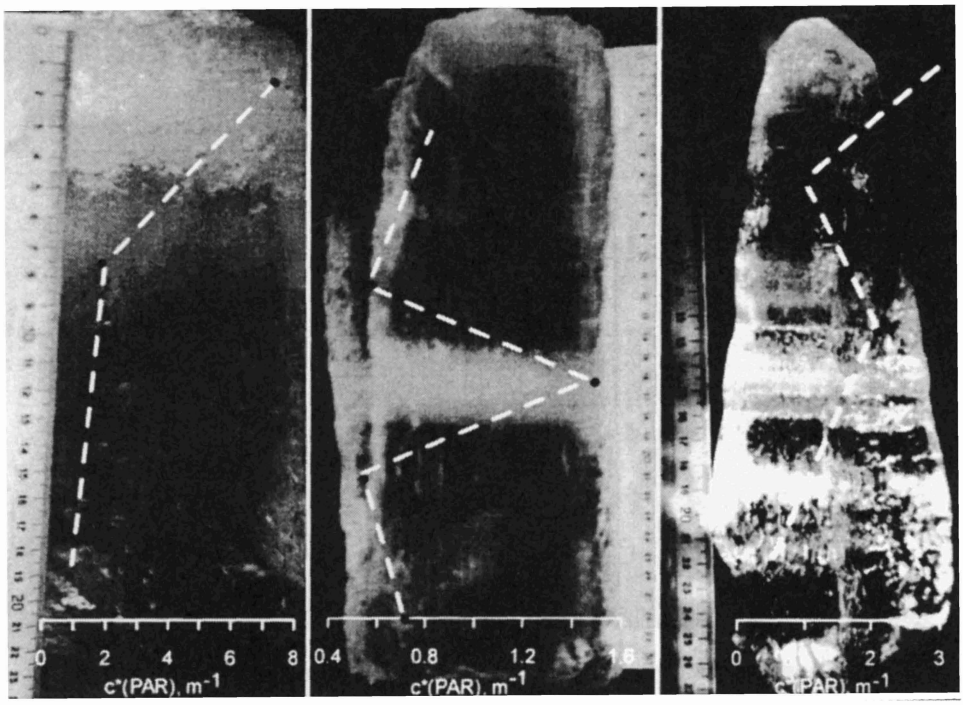

a) b) c)

Fig. 2. Vertical cross-sections of ice structure in winter 2000 (a) Lakes Verevi (28 Feb), (b) Võrtsjärv (1 March), and (c) Maardu (8 March) taken in normal light. PAR attenuation coefficients are also shown.

small crystals (~ 0.1 cm) while the congelation ice was columnar, the size of columns growing with increasing depth. As an example, the ice structure in Lake Harku is presented in Figs. 3a-c. The thick section shows the distribution between snow-ice (5 cm) and congelation ice (17 cm). Snow-ice was fine-grained with one dark line seen at a depth of 4 cm, probably due to earlier surface melting. The transition to columnar ice was very rapid (only a 0.2-0.3 cm transition layer). The columns were 0.5 cm wide and 2-3 cm long, deeper down the dimensions became twice that much.

In Santala Bay the observations were made during 15-30 March. The ice thickness was almost constant over the basin (variation less than 2 cm) but hoarfrost and cracks (larger ones covered by ice) as well as patches of fresh snow and melting dirty snow were found. At the end of March typical whitening of ice cover was noted, likely due to hoarfrost inside the ice. The ice thickness decreased from 29 cm to 21 cm during the observation period. The crystal structure is shown in Figs. 3d-f.

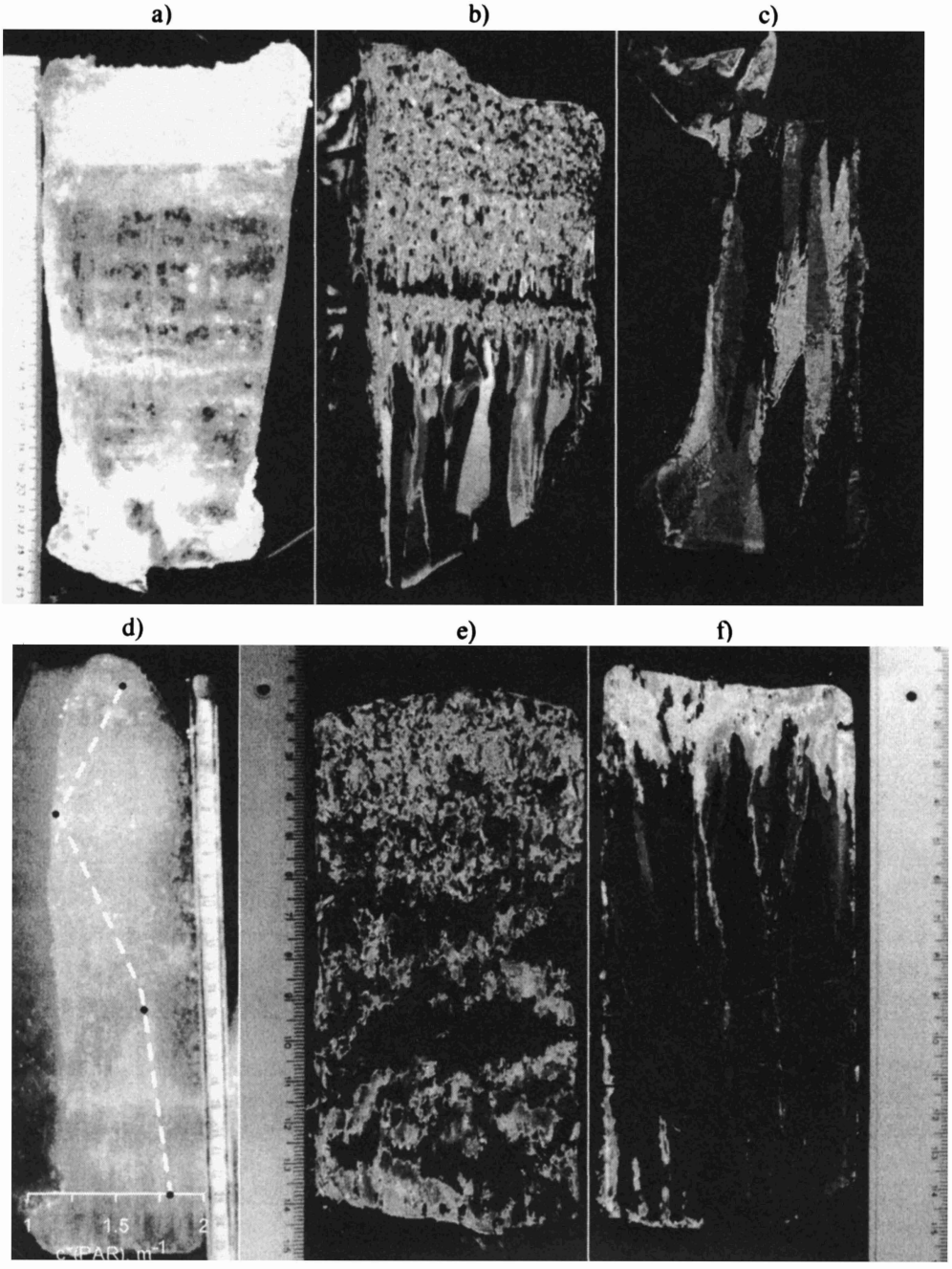

Fig. 3. Ice sample from Lake Harku, 3 March: (a) thick section in normal light, (b-c) thin sections of upper (b) and lower (c) parts in polarized light, and (d-f) analogous photographs for Santala Bay, 16 March, with PAR attenuation coefficient in d.

The thick section was 26.8 cm deep and looked opaque in normal light. The top 13 cm was snow-ice and included many gas bubbles. The lower part was congelation ice, clearer than snow-ice but due to the brine channels much more opaque than in lakes. The thin section show that snow-ice crystal size was 0.05-0.5 cm while the congelation ice consisted of columnar crystals with lengths up to 10 cm and a horizontal size of up to 1 cm. There was no sudden transition into a columnar zone like as the Harku ice sample.

Optical Properties of Ice and Water

During freezing dissolved matter is partly separated from the growing ice into the underlying water. The separation factor is 20-50% in sea water but should be much less in very low salinity lake water (Weeks 1998). Not much is known about the separation of suspended matter. An additional input of impurities comes from atmospheric fallout. The result is that the amount of the yellow substance in meltwater of lake ice is much smaller than in the underlying water, as illustrated by the vertical profiles of the attenuation coefficient c^*_f(380 nm) in Fig. 4. The largest differences were found in eutrophic lakes (Võrtsjärv, Ülemiste); also in the dystrophic N. Mustjärv (not shown in the figure) there was a similar large difference. In these lakes the ratio of c^*_f(380 nm) between water and ice was more than 12, while in the oligotrophic Lake Paukjärv it was only 3.

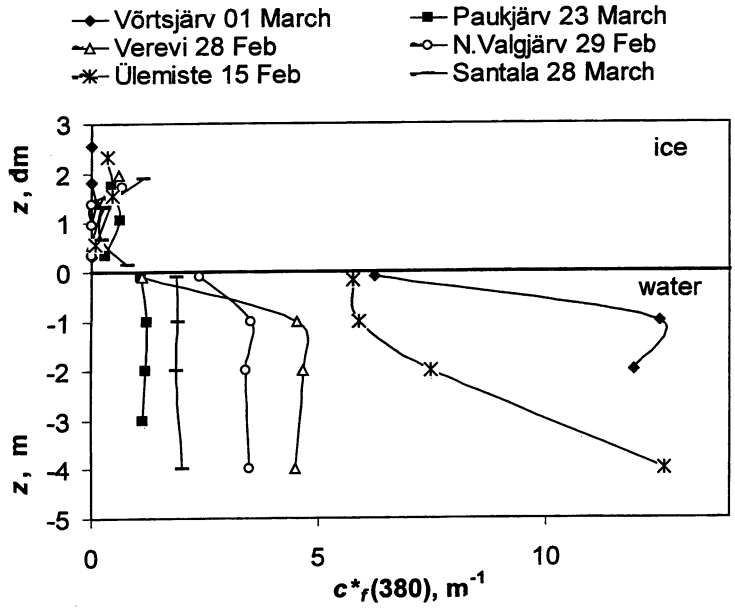

Fig. 4. Examples of vertical profiles of attenuation coefficient c_f^*(380 nm) in and under ice cover. The zero depth refers to the ice bottom, the depth scale in the ice is in decimetres, in the water it is in (negative) metres.

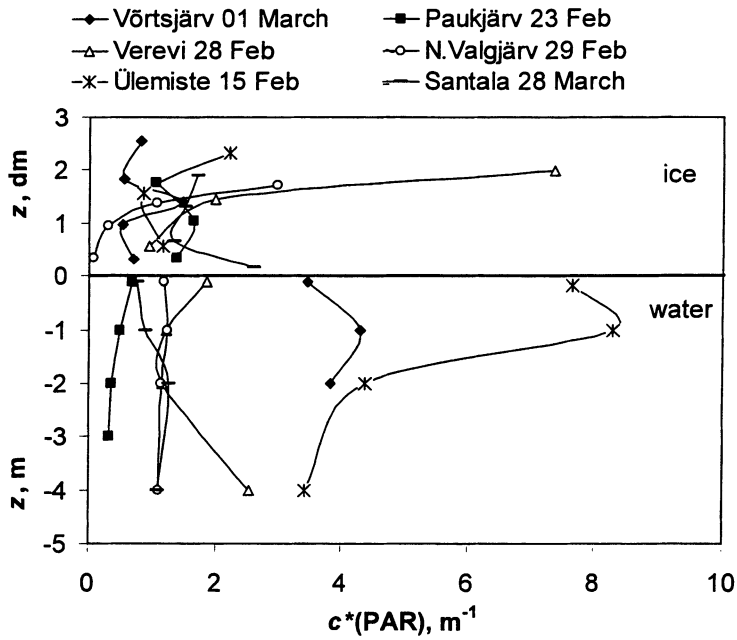

Fig. 5. Examples of vertical profiles of PAR attenuation coefficient in and under ice cover. The zero depth refers to the ice bottom, the depth scale in the ice is in decimetres, in the water it is in (negative) meters.

The PAR-band attenuation coefficient c^*_{PAR} gives a good description of the amount of impurities. Interesting examples of vertical profiles in the ice meltwater are shown in Fig. 2 for lakes Verevi, Võrtsjärv and Maardu. The maxima of c^*_{PAR} are coincident with the opaque ice layers. Atmospheric fallout most probably is the reason for the surface maximum; the attenuation is especially high in Lake Verevi, located in the town of Elva where a lot of houses are heated with wood. The maximum of c^*_{PAR} inside the ice sheet is coincident with maximum chlorophyll *a*. Lake N. Mustjärv ice is comparable with the other lake ice samples but this lake is an extreme example with a very high amount of yellow substance (Arst *et al.* 1996, 1999a).

Fig. 5 gives a general picture of the profiles of the PAR attenuation coefficient. In the eutrophic lakes (Ülemiste, Võrtsjärv) the water beneath the ice is less transparent than the ice meltwater, but in clear water lakes (Paukjärv) the opposite result was obtained. Atmospheric fallout on the ice of clear water lakes causes a higher attenuation coefficient in the ice than in the water. In brackish waters the ice captures more dissolved matter than in lakes. In Santala Bay the ratio of c^*_f(380 nm) between the water and ice was 4. Also the ice meltwater there is less transparent than the water beneath the ice because brackish ice contains brine pockets where phytoplankton may grow.

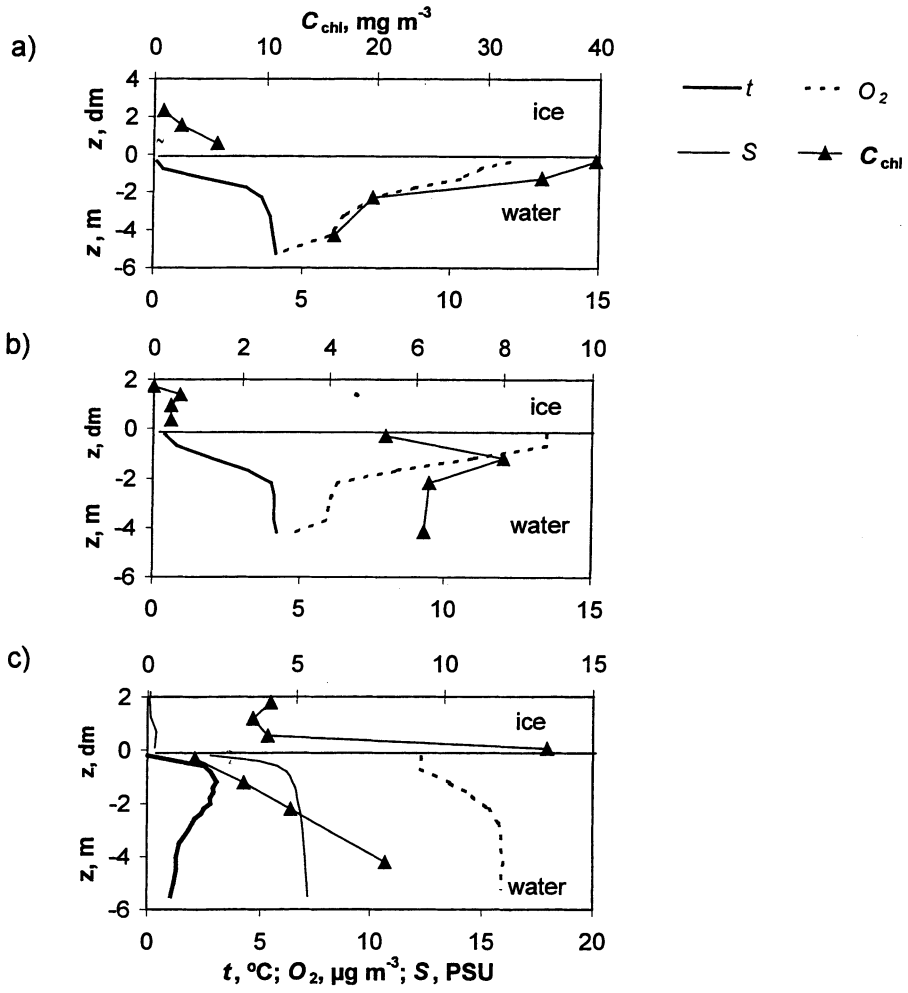

Fig. 6. Vertical profiles of chlorophyll *a* (C_{chl}), temperature *(t)* and dissolved oxygen *(O_2)* in (a) Lake Ülemiste (15 Feb), (b) Nohipalu Valgjärv (29 Feb), and (c) Santala Bay (30 March) in winter 2000. For Santala Bay also salinity (*S*) is given. The zero depth refers to the ice bottom, the depth scale in ice is in decimetres, in water it is in (negative) metres.

Chlorophyll a, Temperature and Oxygen

The chlorophyll *a* level is low in lake ice (0-3 mg m^{-3}) compared with the level in water. Occasionally very high concentrations were measured: *e.g.*, 30.8 mg m^{-3} in Harku on 3 February, maybe due to water in this eutrophic lake flooding onto the ice and freezing. There are three characteristic variants for the vertical distribution of

chlorophyll *a* in ice and the underlying water (Fig. 6). A maximum (39.7 mg m^{-3}) was observed just below the ice in Lake Ülemiste on 15 Feb (Fig. 6a), probably due to the mild winter with a thin ice and snow cover, favouring good light conditions in the water. Often the maximum was found a little deeper, at around 1 m (Lake N. Valgjärv in Fig. 6b). The Santala Bay case is totally different. The lower surface was porous and green-coloured due to algae growth in brine pockets, and the maximum chlorophyll *a* level (13.5 mg m^{-3}) was at the bottom layer of the ice (Fig. 6c); the level of chlorophyll *a* increased with depth in the water.

Lake water temperature increased with depth, and the thermocline was at 2-4 m (examples in Figs. 6a-b). In general the water warmed from January to March just below the ice from 0 to 1.2 °C and at a depth of 2 m from 0.4 to 4.2 °C; the thermocline rose to 1.5 m. During the winter oxygen content decreased quickly from the depth of 0.5-1 m to deeper layers (Figs. 6a-b) where in some cases the minima were dangerously low for living organisms. The conditions varied from virtual anoxia in Lake Verevi (O_2 level less than 2 mg m^{-3}) to supersaturation in the epilimnion of Lake Ülemiste (140%) where phytoplankton started to grow intensively in spring; in Lake Verevi, however, anoxic conditions have been observed also in summertime. Oxygen deficiency in eutrophic lakes under thick ice and snow cover has also been reported by Huttula & Nõges (1998).

At the end of March the water in Santala Bay warmed quickly, from 1.8 to 3.3 °C in two weeks. The maximum temperature was at 1-1.5 m depth, and then the temperature decreased down to 1-2 °C in deeper layers (Fig. 6c). The oxygen level was close to saturation (80-120%), higher values observed in deeper layers where the temperature was lower (Fig. 6c). The oxygen profiles showed a weak minimum at 1 m in depth, then a slight increase and almost constant values in the 2.5-5 m layer. The exchange of water with the Gulf of Finland helped to preserve the oxygen content. The maximum bulk salinity of the ice was 0.45‰ and it decreased in the latter half of March to 0.18‰ since the ice became warmer and brine flowed out. The salinity profile was a weakly inverse c-shape as is normal for spring ice (Fig. 6c). In the water beneath the ice, a sharp thermocline accompanied the halocline. Salinity increased in the first meter from 0.98‰ to 4.89 ‰ and then further to 5.33‰ at the bottom.

Comparison with Ice-free Period

The results for the under-ice water samples can be compared with the long-term ice-free period (May-Oct) data from the same lakes. The range of the concentrations of suspended matter and chlorophyll *a* and attenuation coefficients at 380 nm and PAR band are shown in Table 2. As expected the summer maxima are always remarkably higher than the winter values, but summer minima are comparable with winter minima (in some cases even smaller). The smallest differences were observed for the 380-nm attenuation coefficient except for Lake N. Mustjärv, where its summer values exceeded its winter values 2-5 times.

Table 2 – Minimal and maximal values of water properties under ice cover (in 2000) and in ice-free period (in 1992-1999 from Arst *et al.* 1996, 1999ac).

Water body	Season	C_s (mg L^{-1})	C_{chl} (mg m^{-3})	$c^*_f(380)$, (m^{-1})	c^*(PAR), (m^{-1})
Maardu	Winter	0.4-3.3	3.4-31	0.9-5.8	0.9-1.8
	Summer	0.6-15	6.2-73	4.7-8.4	1.2-6
Harku	Winter	1.0-4.0	5.2-19	15-16	4.2-5.2
	Summer	2.0-176	3.4-1046	9.3-19	4.1-132
Ülemiste	Winter	1.6-6.7	3.9-44	2.1-13	1.9-8.4
	Summer	2.8-34	13-121	3.4-17	4.2-18
Paukjärv	Winter	0.4-0.9	1.1-4.4	1.1-1.2	0.3-0.7
	Summer	0.5-5.2	1.4-11	0.7-1.5	0.6-1.6
Verevi	Winter	1.6-2.4	2.9-7.4	1.1-4.7	1.2-2.5
	Summer	1.0-13	4.4-108	4.6-7.8	1.5-8.7
N.Valgjärv	Winter	1.2-1.6	5.3-8.0	2.4-3.5	1.1-1.3
	Summer	1.0-7.0	0.6-30	1.0-4.5	0.6-4.7
N.Mustjärv	Winter	2.4	8.4	18	5.0
	Summer	2.0-16	1.7-46	38-93	13.7-21
Võrtsjärv	Winter	3.0-3.8	2.5-5.0	5.5-10	3.4-4.3
	Summer	5.0-145	23-102	6.2-12	3.3-28
Santala Bay	Winter	1.3-3.9	1.6-19	1.2-3.9	0.6-1.4

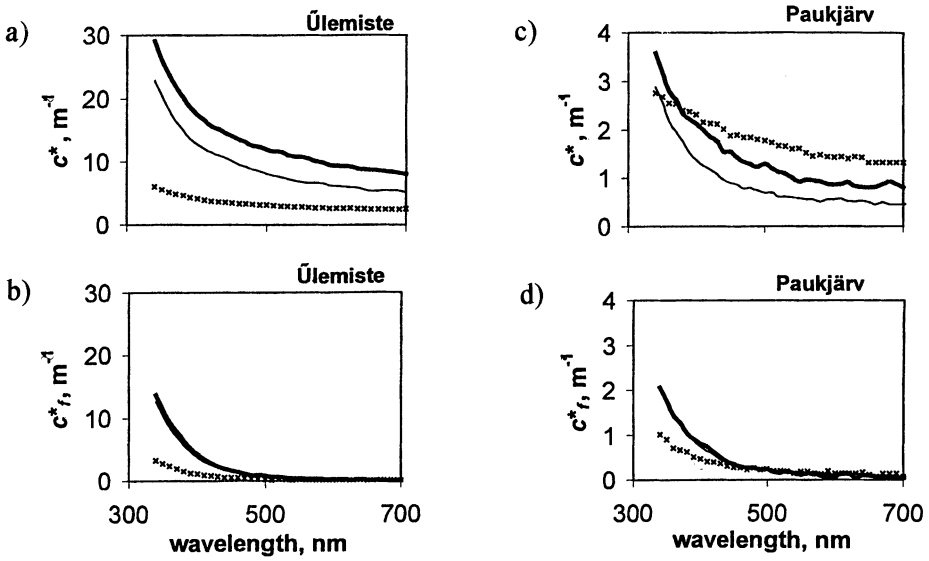

Fig. 7. Spectra of attenuation coefficients of unfiltered water and filtered water, c^* and c_f^*, in (a-b) Lake Ülemiste and (c-d) Lake Paukjärv. Crosses – ice meltwater; thin line – winter (Feb) water sample; solid line – summer (June) water sample.

Examples of the spectral attenuation coefficients of unfiltered and filtered water samples are shown in Fig. 7 for the turbid Lake Ülemiste and the clear Lake Paukjärv. Unfiltered water shows smaller light attenuation in winter than in summer for both lakes due to the difference in the amount of suspended particles. Filtered waters (lower plots of Fig. 7) give practically coincident result in summer and winter, which means that there is a more or less a fixed all-year amount of yellow substance.

Solar Radiation

Albedo and Transmittance of Ice Cover

At latitudes 58°-60° N winter is characterised by short days and large solar zenith angles (56°-83° for our measurements), which cause low values of incident PAR. We had a clear sky only on 28 and 29 March, in other cases the sky was partially or even totally cloudy (28, 29 Feb; 17, 18, 23, 30 March). The diurnal maximum incident downwelling irradiance varied about tenfold during the experimental period (110-1,310 μmol m^{-2} s^{-1}) while the downwelling irradiance 0.5 m below the ice was 1.4-286 μmol m^{-2} s^{-1}.

Albedo measurements were made in Santala Bay where the ice surface conditions varied from melting wet ice to refrozen snow patches (Table 1). PAR albedo was 0.28-0.76, being lowest for ice covered by a thin water layer and highest for snow patches. Fresh snow albedos were typically high (0.8-0.9) and constant in the PAR band as reported earlier for Santala Bay by Rasmus *et al.* (2002). The albedo of deteriorated snow had a weak maximum at 550 nm with the overall level above 0.4.

Light transmittance in the PAR band (T_{PAR}) through the ice/snow sheet was most strongly affected by the presence of snow cover (Table 3). Depending on the snow thickness the transmittance varied from 1 to 10%, increasing about seven times when the snow was removed. With a thin layer of water on the ice the transmittance increased and varied only slightly (37-41%) in different lakes. The transmittance of brackish ice in Santala Bay varied from 15% with melting snow patches to 52% for 15 cm clear ice. Fritsen and Priscu (1999) showed that often in spring an additional attenuation of PAR inside the ice is observed due to ice whitening (hoarfrost, increase of brine volume, phytoplankton bloom inside the ice). A rapid increase in transmission occurs only during the latter half of spring when the ice is thin and contains a lot of water.

Characteristics of the Solar Light Field under the Ice Cover

The plane and scalar diffuse attenuation coefficients K_d(PAR) and K_0(PAR) describe the vertical transfer of PAR from the surface down to deep layers inside the water column. There were large differences between the investigated water bodies (Table 3): K_d(PAR) was one order of magnitude smaller in Lake Paukjärv (clearest) than in

Table 3 – Characteristics of the solar light field under the ice cover by the data obtained in winter 2000. The results obtained on the same day, but at different times, are averaged, limits show the variation during the measurement period.

Water body	thickness (cm)		T(PAR) %	K_d (PAR), m^{-1}	K_o (PAR), m^{-1}	E_d/E_o (0-)	$E_o(0.5)/E_d$(air), %	$E_d(0.5)/E_d$(air), %
	ice	snow						
Harku	22	2	1	1.3	1.9	0.30	0.5	1.0
	22	-	4	2.1	2.6	0.35	1.2	2.3
Ülemiste	22-27	1-6	2-10	1.0-1.7	1.7	0.42	1.4-5.6	11
	22-27	-	13-37	1.7-1.9	1.6-2.1	0.42-0.52	7.6-18	21
Paukjärv	21	6	3	0.3	-	-	2.9	-
	21	-	22	0.8	-	-	18	-
Verevi	22	-			0.9	-		34
N.Valgjäv	19	-	41	0.7	1.0	0.66	23	34
Võrtsjärv	30	-	40	1.4	1.3	0.58	23	37
Maardu	28	-	37	0.9	1.0	0.62	18	36
Santala Bay	15-29	-	15-52	0.5-0.9	0.7-1.0	0.55-0.75	12-35	14-43

Lake Ülemiste (turbid). The diffuse attenuation coefficients were usually within the range measured during the ice-free period (overview in Arst *et al.* 1999b-c). They were remarkably lower in winter only in Lake Harku (ice-free limits K_d(PAR) ~ 8.8-14.9 m^{-1} and K_0(PAR) ~ 8.5-13.2 m^{-1}) and in Lake Paukjärv (ice-free limits K_d(PAR) ~ 3.0-8.3 m^{-1} and K_0(PAR) ~ 2.6-6.3 m^{-1}). This corresponds to the relatively low concentrations of OAS in winter (Table 2). Removing the snow increased the attenuation coefficients by the factor of 1.1-2.6, because snow is a highly scattering substance and the radiation penetrating through snow is much more diffuse. Also, *e.g.*, K_d(PAR) is higher for direct solar beams at zenith angles greater than 38° than for a diffuse light field (Kirk 1984).

There is a strong correlation between the plane and scalar diffuse attenuation coefficients (R=0.91; N=12; p<0.0001) but K_0(PAR) is about 10% higher. In open water conditions in same water bodies the opposite is true: K_d(PAR) is about 10% higher (Reinart and Herlevi 1999). It should be noted that winter measurements were performed only to depth of 1.5 m and K_o(PAR) probably does not decrease so quickly in deeper layers.

The vertical profiles of the diffuse attenuation coefficients were estimated from the irradiance data at 0.25-m step: $K_{d,o} = 4\ m^{-1} \times \ln[E_{d,o}(z_1)/E_{d,o}(z_2)]$ where E is irradiance. In the lakes with varying amounts of OAS and with measurements made over a longer period these profiles showed variability: typically the attenuation coefficient decreased with increasing depth, but occasionally the opposite result was obtained. The latter cases (*e.g.*, Fig. 8b) probably show the increase of OAS with depth (in homogeneous water both coefficients should decrease with depth). By our measurements the increase of K_d(PAR) with depth is accompanied with a remarkable in-

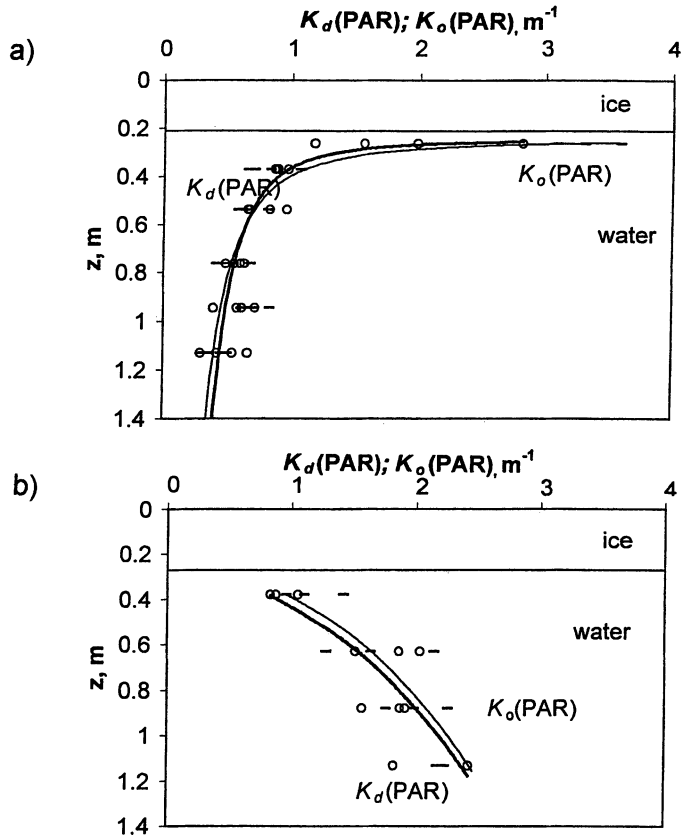

Fig. 8. Vertical profiles of plane and scalar diffuse attenuation coefficients K_d(PAR) (trace) and K_o(PAR) (rings) in steps of 0.25 m: (a) Santala Bay 30 March, and (b) Lake Ülemiste 23 March. Thin line represents the power law fit for K_o(PAR) and the solid line is the same for K_d(PAR).

crease of the concentrations of suspended matter and chlorophyll *a* as well as the beam attenuation coefficient. In Santala Bay the diffuse attenuation coefficients decreased with increasing depth (a typical example is shown in Fig. 8a).

The parameter describing the angular distribution of under-ice light field is the ratio of plane and scalar irradiances E_d/E_o, measured, respectively, by a planar cosine sensor and a spherical sensor (Table 3). It depends on the incident solar irradiance, solar zenith angle, and absorption and scattering coefficients (Bannister 1992). As we go deeper into the water column the effect of the surface conditions becomes negligible, inherent optical properties prevail, and in homogeneous water the apparent optical properties reach asymptotic values. The ratio E_d/E_o is rather close to the average cosine of the light field since the upwelling light stream does not exceed E_d by more than a few percent in these waters (Arst *et al.* 1996).

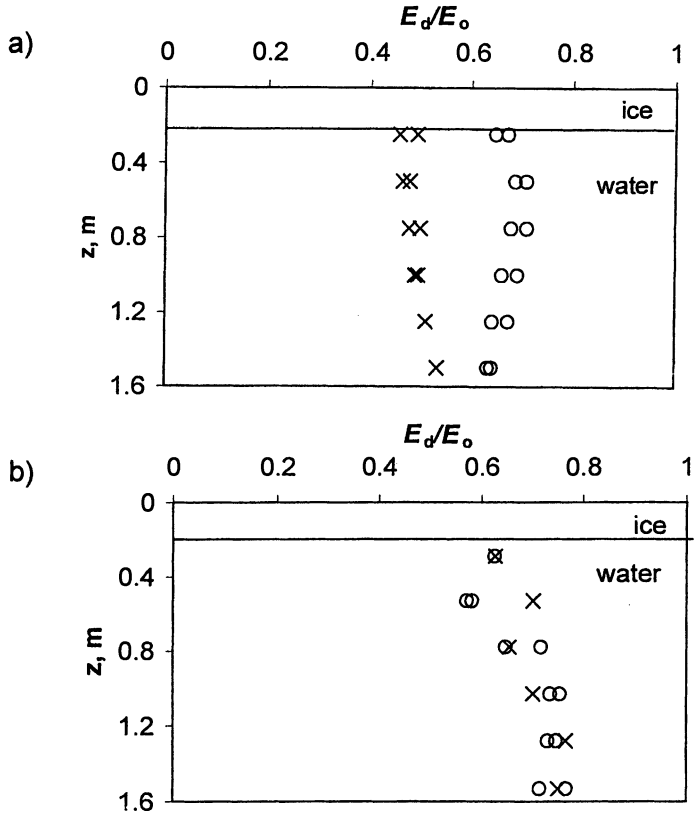

Fig. 9. Vertical profiles of the ratio of plane to scalar irradiance E_d/E_o measured in one position of sensors (crosses) and on the same point, but turning sensors 180° (rings): (a) Santala Bay 28 March, and (b) Lake Maardu 08 March.

Fig. 9a is a good example showing how the four vertical profiles of E_d/E_o (these describe two pairs of measurements with sensors turned 180°, see Fig. 1) move closer to each other with depth. In most cases E_d/E_o increased slightly with depth (Fig. 9b). A low value just under the ice (0.30) was measured in Lake Harku (3 March) in conditions of low sun and snow cover on the ice. Midday summer measurements show higher ratios, Reinart and Herlevi (1999) measured values of 0.43-0.90. Then the incident irradiance is mostly formed by sunrays, the light field becomes more diffuse deeper in the water, and a decrease of E_d/E_o with depth results. Low values are expected under ice (as shown by Berwald *et al.* 1995) since in a highly scattering environment (in an ice layer a single scattering albedo is more than 0.95) the asymptotic average cosine of the light field is less than 0.42. The complicated depth profile of the average cosine (and increase with depth) is a result of "broadening" the radiance distribution (Bannister 1992).

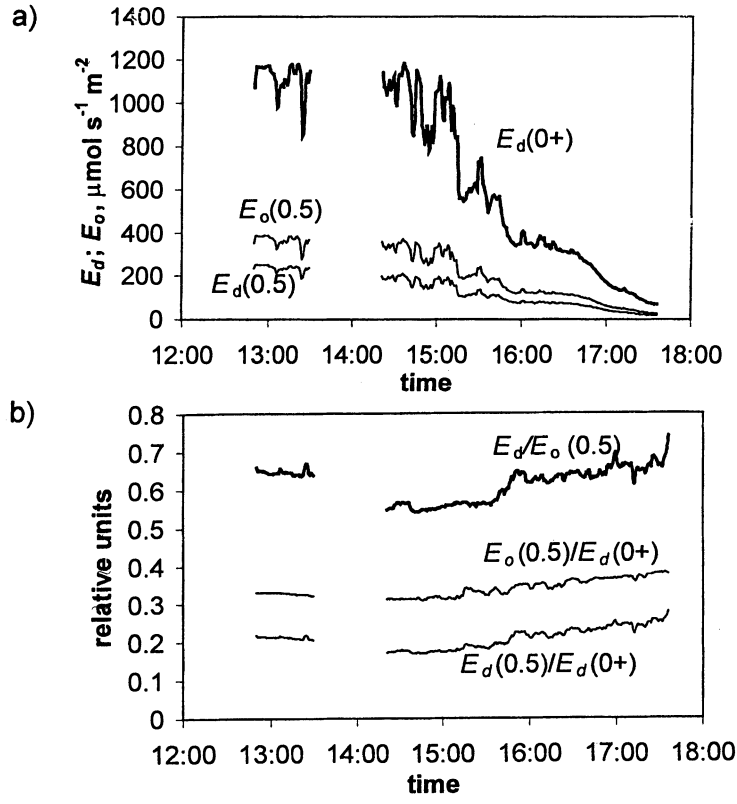

Fig. 10. Diurnal variation of radiation characteristics: (a) PAR, incident on the ice surface (solid line) and at 0.5 m below the ice (thin lines); (b) Ratio of plane to scalar irradiance E_d/E_o (solid line) and portions of E_d and E_o from incident PAR (thin lines) at 0.5 m below the ice. A break in recording was made for vertical profiling around midday.

Depending on ice and weather conditions the level of PAR at 0.5 m beneath the ice varies (Table 3). The relative plane irradiance was smallest (0.5%) in Harku, on 3 February and highest (35%) in Santala Bay on 18 March. However, because of the diffuseness of the light field there is actually more light available for photosynthesis in water: the scalar irradiance is at a depth of 0.5 m, 1-43% from the incident irradiance. There is also diurnal variation in the light field (Fig. 10). Continuous measurements for one day showed that the ratio E_d/E_o increased as the sun's elevation decreased and the portion of irradiance incident on the surface and penetrating the ice layer slightly increased. This is caused by the increase of the amount of diffuse light in total incident irradiance with solar zenith angle. The reflection of the direct solar radiation increases while the reflection of the diffuse component is almost the same until the sun goes down.

Attenuation of PAR determines the depth where photosynthesis is still possible under the ice cover. Commonly the euphotic depth is taken as the depth where PAR level is 1% of the incident PAR. This depth was smallest (0.1 m) in Lake Harku with 2-cm snow cover and about 5.5 m in Lake N. Valgjärv. In Santala Bay it varied from 4.2 to 7.2 m depending on surface features. Thus under bare ice cover there are relatively good light conditions for phytoplankton growth but snow cover reduces the light remarkably. The euphotic depth in Estonian lakes during summer is 0.4-12 m. However, the temperature and stratification are totally different in winter thus changing conditions for phytoplankton growth, and this situation needs further investigation.

Conclusions

To understand the factors influencing the ecological state of ice-covered water bodies, a field programme was performed on under-ice light fields and the optical properties of ice, ice meltwater and water beneath ice. Observations were made in the mild winter of the year 2000 in eight Estonian lakes and in one brackish water basin, Santala Bay in the Gulf of Finland. A new system designed for the optical measurements beneath the ice was successfully tested. Our data bank for winter conditions is still small and our investigations will continue. The following conclusions were drawn:

1) There are large differences between the properties of fresh and brackish water ice (ice structure, amount of particles, and dissolved matter), which influence the underwater light field. The vertical profiles of temperature and dissolved oxygen in the lakes and in Santala Bay are also different.
2) Despite temporal changes in the properties of ice, the most important factor affecting the albedo and transmittance of ice is the snow cover. Ice surface PAR albedo was 0.28-0.76, lowest for ice covered by thin water layers and highest for snow patches. Ice cover transmittance by the presence of snow is low (1-10%) but more without snow (4-52%).
3) The amount of yellow substance in lake ice is very small in comparison to that in the underlying water. The largest differences occur in eutrophic and dystrophic lakes. In Santala Bay the chlorophyll *a* concentration has its maximum in the bottom layer of ice, but in the lakes it is mostly just under the ice or a little deeper. In eutrophic lakes the beam attenuation coefficient is greater in the water than in the ice, but in clear waters (Lake Paukjärv, Santala Bay) the opposite is true. Lake ice may contain a lot of particles, but this is affected more by atmospheric fallout than the water impurities.
4) The light field in the water is much more diffuse under snow and ice cover than in open water conditions. Therefore PAR available for photosynthesis (scalar ir-

radiance) is higher than PAR measured by the plane sensors widely used in limnology. According to our measurements the ratio of plane to scalar irradiance under ice is 0.30-0.75, which is smaller than in summer conditions (0.43-0.90). Plane and scalar diffuse attenuation coefficients K_d(PAR) ~ 0.3-2.1 m^{-1} and K_o(PAR) ~ 0.7-2.6 m^{-1} are close to the lower limit in ice-free period in the same lakes.

5) In winter the water is much more clear than in summer because biological activity and inflow from the shore is hindered. The concentrations of suspended matter and chlorophyll *a* as well as the beam attenuation coefficient under the ice are comparable with the minima and remarkably lower than maxima in the ice-free period.
6) Biological activity and the spring warming under the ice begin much before the ice actually melts. The winter euphotic depth was smallest (0.1 m) in the eutrophic Lake Harku with snow on the ice and much larger (5.5 m) in clear water lakes. If the ice is snow free, the euphotic depth is within the limits of summer conditions. Despite this, some depletion of oxygen was observed in lakes.

Acknowledgements

We wish to thank the Kalle, Vilho and Yrjö Väisälä Foundation of the Academy of Science of Finland and Estonian Science Foundation (grant 3613) for financial support for this investigation. The authors are indebted to Mats Granskog for help in the work with ice thin sections and Antti Lindfors for salinity data. Mr. Donald Smart is thanked for checking the English.

References

Allison, I., Brandt, R. E., and Warren, S. G. (1993) East Antarctic sea ice: Albedo, thickness distribution and snow cover, *J. Geophys. Res.,Vol. 98*, pp. 12417-12429.

Arrigo, K. R., Sullivan, C. W., and Kremer, J.N. (1991) A biological model of Antarctic sea ice, *J. Geophys.Res., Vol. 96*, pp. 10581-10592.

Arst, H., Mäekivi, S., Kutser, T., Reinart, A., Blanco-Sequeiros, A., Virta, J., and Nõges, P. (1996) Optical Investigations of Estonian and Finnish lakes, *Lakes and Reservoirs: Research and Management, Vol. 2*, pp. 187-198.

Arst, H., Erm, A., Kallaste, K., and Mäekivi, S. (1999a) Influence of the conditions of preserving water samples and their delayed processing on the light attenuation coefficient spectra and the concentrations of water constituents, *Proc. Estonian Acad. Sci. Biol. Ecol., Vol. 48 (2)*, pp. 149-160.

Arst, H., Erm, A., Kallaste, K., Mäekivi, S., Reinart, A., Herlevi, A., Nõges, T., and Nõges, P. (1999b) Investigation of Estonian and Finnish lakes by optical measurements in 1992-1997, *Proc. Estonian Acad. Sci. Biol. Ecol.,Vol. 48 (1)*, pp. 5-24.

Arst, H., Erm, A., Kutser, T., and Reinart, A. (1999c) Optical remote sensing and contact measurements in Estonian and Finnish lakes in 1992-98, 4th Workshop on Physical Processes in Natural Waters. Rep. Series. Estonian. Marine Inst. 10, pp. 105-110.

Bannister, T.T. (1992) Model of the mean cosine of underwater radiance and estimation of underwater scalar irradiance, *Limnol. Oceanogr., Vol. 37*, pp. 773-780.

Berwald, J., Stramski, D., Mobley, C. D., and Kiefer, D. A. (1995) Influences of absorption and scattering on vertical changes in the average cosine of the underwater light field, *Limnol. Oceanogr., Vol. 40*, pp. 1347-1357.

Fritsen, C. H, and Priscu, J. C. (1999) Seasonal change in the optical properties of the permanent ice cover on Lake Bonney, Antarctica: Consequences for lake productivity and phytoplankton dynamics *Limnol. Oceanogr., Vol. 44 (2)*, pp. 447-454.

Granberg, H. B. (1998) Snow cover on sea ice. In: M. Leppäranta (ed): *Physics of ice-covered seas*, pp. 605-651. Helsinki: Helsinki University Printing House.

Huttula, T., and Nõges, T., eds. (1998) Present state and future fate of Lake Võrtsjärv. Results from Finnish-Estonian joint project in 1993-1997. Tampere, Finland: Multiprint.

Jerlov, N. G. (1968) *Optical Oceanography,* Elsevier Oceanography Series, No. 5, pp. 194 p.

Kirk, J. T. O. (1984) Volume scattering function, average cosines, and the underwater light field, *Limnol. Oceanogr., Vol. 29 (2)*, pp. 350-356.

Kutser, T., Veismann, U., Reinart, A., Erm, A., Herlevi, A., and Kallio, K. (1999) Field performance of the ST 1000 spectrometer in passive optical remote sensing of water bodies, *Proc. Estonian Acad. Sci. Biol. Ecol., Vol. 48 (1)*, pp. 37-46.

Leppäranta, M., Tikkanen, M., and Shemeikka, P. (1998) Observations of ice and its sediments on the Baltic coast, *Nord.Hydrol., Vol. 29*, pp. 199-220.

Michel, B., and Ramseier, R. O. (1971) Classification of river and lake ice, *Can. Geotech.J., Vol. 8 (13)*, pp. 36-45.

Palosuo, E. (1963) The Gulf of Bothnia in winter. II. Freezing and ice forms, *Merentutkimuslait. julk./Havsforskningsinst., Skr. 208,* Helsinki

Perovich, D.K. (1998) The optical properties of the sea ice. In: M. Leppäranta (ed): *Physics of ice-covered seas*, pp. 195-230. Helsinki: Helsinki University Printing House.

Rasmus, K., Ehn, J., Granskog, M., Kärkäs, E., Leppäranta, M., Lindfors, A., Pelkonen, A., Rasmus, S., and Reinart, A. (2002) Optical measurements of sea ice in the Gulf of Finland, *Nord. Hydrol.*, Vol. *33 (2/3)*, pp. 207-226.

Reinart, A., Arst, H., Blanco-Sequeiros, A., and Herlevi, A. (1998) Relation between underwater irradiance and quantum irradiance in dependence on water transparency at different depths in the water bodies, *J. Geophys. Res., Vol. 103*, pp. 7749-7752.

Reinart, A., and Herlevi, A. (1999) Diffuse attenuation coefficient in some Estonian and Finnish lakes, *Proc. Estonian Acad. Sci. Biol. Ecol., Vol. 48 (4)*, pp. 267-283.

Russak V. (1990) Air temperature (in Estonian). *Climate of Tartu and its Changes during the Recent Decades*, pp. 76-88, Tartu, Estonia

Tooming, H., and Kadaja, J. (1995) Changes in snow cover and surface albedo in Estonia during the last 100 years, *Meteorologische Zeitschrift, 8*, pp. 6-21.

Weeks, W. F. (1998) Growth conditions and the structure of sea ice. In: M. Leppäranta (ed): *Physics of ice-covered seas*, pp. 5-105. Helsinki: Helsinki University Printing House.

Received: 24 April, 2001
Revised: 8 July, 2002
Accepted: 2 September, 2002

Addresses:
Matti Leppäranta,
Division of Geophysics,
University of Helsinki,
P.O.Box 64,
FI-00014 Helsinki,
Finland.
Email: Matti.Lepparanta@phnet.Fi

Anu Reinart, Ants Erm, Helgi Arst,
Medhat Hussainov and Liis Sipelgas,
Marine Systems Institute
at Tallinn Technical University,
Paldiski Road 1,
10137 Tallinn,
Estonia.
Email: anu.reinart@ebc.uu.se
helarst@online.ee